

ARMY RESEARCH LABORATORY



Polymer Materials for Ground Mobile Millimeter-Scale Robotics

by Ryan Rudy, Ronald G. Polcawich, and Jeff Pulskamp

ARL-TR-4659

December 2008

NOTICES

Disclaimers

The findings in this report are not to be construed as an official Department of the Army position unless so designated by other authorized documents.

Citation of manufacturer's or trade names does not constitute an official endorsement or approval of the use thereof.

Destroy this report when it is no longer needed. Do not return it to the originator.

Army Research Laboratory

Adelphi, MD 20783-1197

ARL-TR-4659

December 2008

Polymer Materials for Ground Mobile Millimeter-Scale Robotics

Ryan Rudy, Ronald G. Polcawich, and Jeff Pulskamp
Sensors and Electron Devices Directorate, ARL

REPORT DOCUMENTATION PAGE*Form Approved*
OMB No. 0704-0188

Public reporting burden for this collection of information is estimated to average 1 hour per response, including the time for reviewing instructions, searching existing data sources, gathering and maintaining the data needed, and completing and reviewing the collection information. Send comments regarding this burden estimate or any other aspect of this collection of information, including suggestions for reducing the burden, to Department of Defense, Washington Headquarters Services, Directorate for Information Operations and Reports (0704-0188), 1215 Jefferson Davis Highway, Suite 1204, Arlington, VA 22202-4302. Respondents should be aware that notwithstanding any other provision of law, no person shall be subject to any penalty for failing to comply with a collection of information if it does not display a currently valid OMB control number.

PLEASE DO NOT RETURN YOUR FORM TO THE ABOVE ADDRESS.

| | | | | | |
|---|-------------|---------------------------|-------------------------------|--|---|
| 1. REPORT DATE (DD-MM-YYYY) December 2008 | | 2. REPORT TYPE Summary | | 3. DATES COVERED (From - To) May to August 2008 | |
| 4. TITLE AND SUBTITLE Polymer Materials for Ground Mobile Millimeter-Scale Robotics | | | | 5a. CONTRACT NUMBER | |
| | | | | 5b. GRANT NUMBER | |
| | | | | 5c. PROGRAM ELEMENT NUMBER | |
| 6. AUTHOR(S) Ryan Rudy, Ronald G. Polcawich, and Jeff Pulskamp | | | | 5d. PROJECT NUMBER | |
| | | | | 5e. TASK NUMBER | |
| | | | | 5f. WORK UNIT NUMBER | |
| 7. PERFORMING ORGANIZATION NAME(S) AND ADDRESS(ES) U.S. Army Research Laboratory ATTN: AMSRD-ARL-SE-RL 2800 Powder Mill Road Adelphi, MD 20783-1197 | | | | 8. PERFORMING ORGANIZATION REPORT NUMBER ARL-TR-4659 | |
| 9. SPONSORING/MONITORING AGENCY NAME(S) AND ADDRESS(ES) | | | | 10. SPONSOR/MONITOR'S ACRONYM(S) | |
| | | | | 11. SPONSOR/MONITOR'S REPORT NUMBER(S) | |
| 12. DISTRIBUTION/AVAILABILITY STATEMENT Approved for public release; distribution unlimited. | | | | | |
| 13. SUPPLEMENTARY NOTES | | | | | |
| 14. ABSTRACT This project is closely tied with the ongoing work of visiting Professor Kenn Oldham and the U.S. Army Research Laboratory's (ARL) joint effort on creating highly flexible, large payload capacity joints for a ground mobile millimeter-scale robot. The fabrication process to add parylene coatings to the piezo-microelectromechanical systems (piezoMEMS) actuator process has been characterized using test structures. Scanning electron and optical microscopy of the joint assemblies; analysis of the coating technology for trench fill; process robustness to exposure to solvents and photolithographic processing; and adhesion of parylene to both platinum and lead zirconate titanate (PZT) thin films have been completed on two separate fabrication sequences. Parylene coatings have been successfully applied to both platinum and PZT thin films and the challenges associated with parylene survival with multiple fabrication process steps have been evaluated. Future work will include full release of test structures on the existing wafers in fabrication as well as implementation of process improvements into a fully functional piezoMEMS plus parylene actuator joint. | | | | | |
| 15. SUBJECT TERMS Parylene, polymer materials, mm-scale robotics | | | | | |
| 16. SECURITY CLASSIFICATION OF: | | | 17. LIMITATION OF ABSTRACT | 18. NUMBER OF PAGES | 19a. NAME OF RESPONSIBLE PERSON |
| a. REPORT | b. ABSTRACT | c. THIS PAGE | UU | 22 | Ronald G. Polcawich |
| U | U | U | | | 19b. TELEPHONE NUMBER (Include area code) (301) 394-1275 |

Standard Form 298 (Rev. 8/98)
Prescribed by ANSI Std. Z39.18

Contents

| | |
|---|-----------|
| List of Figures | iv |
| Acknowledgments | v |
| 1. Introduction/Background | 1 |
| 2. Experiment | 2 |
| 3. Results and Discussion | 4 |
| 3.1 Trench Junctions..... | 4 |
| 3.2 Parylene Adhesion and Etching | 7 |
| 3.3 Trench Analysis..... | 8 |
| 3.4 Photolithography | 10 |
| 4. Conclusions | 11 |
| 5. References | 12 |
| Acronyms | 13 |
| Distribution List | 14 |

List of Figures

| | |
|---|----|
| Figure 1. The conceptual design of the ground mobile millimeter-scale robot highlighting various components and systems required for operation..... | 1 |
| Figure 2. Parylene fabrication process: 1. Pattern (dummy) actuators; 2. Etch deep trenches; 3. Coat parylene; 4. Deposit oxide hard mask; 5. Pattern photoresist for parylene etch; 6. Etch parylene and photoresist; 7. Deposit additional oxide; 8. Pattern oxide, thin photoresist; 9. Etch deep trenches; and 10. XeF ₂ release. | 3 |
| Figure 3. The sample actuator/flexure/leg-link test structure. In figures 4–8 the structures also contain a D-Flexure in parallel to the flexure..... | 4 |
| Figure 4. This photograph from the optical microscope illustrates failure at the junction between the flexure and the leg link possibly from improper parylene fill or photoresist bubbles. | 5 |
| Figure 5. This photograph from the optical microscope illustrates a failure at the junction between the D-flexure and the anchor possibly from improper parylene fill or photoresist bubbles. | 5 |
| Figure 6. This photograph from the optical microscope shows insufficient parylene fill in the dark black areas near the four-trench junction at the anchor and D-Flexure intersection. | 6 |
| Figure 7. This photograph from the optical microscope shows insufficient parylene fill in the dark black areas near the Flexure-leg link four-trench junction. | 7 |
| Figure 8. Surface residue on exposed silicon after anisotropic oxygen plasma RIE Lam 590..... | 8 |
| Figure 9. This photograph from the SEM shows a parylene filled trench 5 μm wide. The etch depth here is approximately 82 μm. | 9 |
| Figure 10. This photograph from the SEM shows the parylene filled trenches of widths of 3, 4, 5, 6, and 7 μm spaced 30 μm apart. The etch depth is approximately 76 μm for the 5 μm wide trench. | 9 |
| Figure 11. The graph shows that trenches that are close together result in more shallow etch profiles and that trench depth is linearly dependent on trench width within the range of etch..... | 10 |

Acknowledgments

The authors would like to acknowledge Richard Piekarz, Joel Martin, and Eugene Zakar of the Sensors and Electron Devices Directorate, U.S. Army Research Laboratory and Brian Power of General Technical Services.

INTENTIONALLY LEFT BLANK.

1. Introduction/Background

There has recently been a push within the U.S. Army Research Laboratory (ARL) to create ground mobile millimeter-scale robotics for surveillance purposes. Current challenges are faced in fabrication due to the relatively large amount of weight the base structure must support. This weight is due to power systems, control systems, and communications systems as well as any other additional components, as seen in the conceptual design in figure 1 (1).

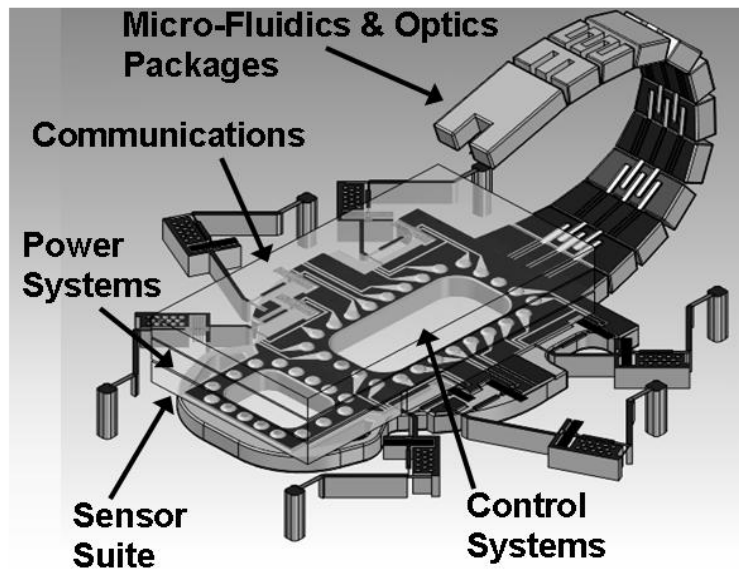


Figure 1. The conceptual design of the ground mobile millimeter-scale robot highlighting various components and systems required for operation.

In order to address this issue, high aspect ratio leg links will be fabricated to increase the weight bearing capabilities. Previous work has been done in designing and processing such devices with a protective parylene skeleton as well as flexible parylene joints. Parylene was chosen because it can provide uniform coatings within deep narrow spaces, allowing for the coating of large aspect ratio trenches for the leg links. Parylene also provides the flexibility needed to create leg links with a large range of motion (2).

Initial process integration and characterization was done to determine a proper fabrication process; however, the yield of successful test structures was low. Problems arose in the first round of fabrication because the protective parylene was etched through so that during the final release step, the silicon etch that was supposed to be protected was instead etched away. The photolithography mask was revised in an attempt to prevent this occurrence with other wafers. Further hypothesized problems include keyholes forming when the top of the trench is closed

before the trench is filled during the parylene deposition in the deep trenches of the leg link structure. The wafers from the first fabrication run have been analyzed and more wafers are being processed to duplicate or improve upon the results found.

2. Experiment

Test structures from the first fabrication run performed by Dr. Kenn Oldham were diced and analyzed using scanning electron microscopy (SEM). To ensure the charging of the parylene would not affect the quality of the SEM images, a thin coating of sputtered gold was added to each test structure. Trenches of various widths that had been filled with parylene were of particular interest to determine if keyholes had formed during deposition. In addition to the SEM, these test structures were photographed using the optical microscope to look for defects and flaws in the parylene coating, especially at the intersection junction of critical features.

In order to perform testing of the parylene fabrication process, prototype test actuators were made from silicon dioxide, platinum-coated silicon dioxide, or a lead zirconate titanate (PZT) stack; all approximately 5000 Å thick. These structures are patterned to represent the size and shape of piezoelectric actuators used to create large in-plane rotational joints. The silicon dioxide test actuators were deposited using a plasma-enhanced chemical vapor deposition (PECVD) process to achieve a depth of approximately 5000 Å, and then patterned and etched via reactive ion etching (RIE). The platinum-coated silicon dioxide test actuators were formed by first depositing 5000 Å of silicon dioxide via PECVD and then sputtering a 200 Å titanium adhesion layer followed by an 820 Å platinum layer. This was then patterned and etched using ion milling and RIE. The PZT layers were deposited as described in section 1, and then patterned and etched using ion milling and RIE.

After deposition and subsequent patterning of these test actuators, narrow trenches were etched into the silicon wafer with deep RIE (DRIE). The etch depth was one of the critical features to assess during this characterization and was varied from 75 to 300 μm. To characterize the trench etch depth, a Tencor Stylus profilometer was used to measure wide features (~150 μm) to give an assessment of the etch depth in the narrow trenches. The narrow features can be measured with conventional metrology tools such as optical and stylus profilometry. Furthermore, RIE lag severely degrades the etch rate in high aspect ratio narrow trenches; therefore, measuring the wider features only gives an estimate of the etch depth. Accurate measurements are performed using cross-section SEM measurements after fabrication.

Following the silicon DRIE, the wafer is then coated with hexamethyldisilazane (HMDS) and loaded into a parylene deposition system. The parylene is deposited to a thickness of approximately 7 μm in order to fill the trenches. After the parylene coating, a 100 nm thick silicon dioxide is deposited with a low-temperature PECVD at 160 °C. The silicon dioxide is

then patterned and etched using RIE with a fluorinated plasma, and serves as a hard mask for the removal of parylene via an oxygen plasma etch. After the exposed parylene has been removed, a second layer of PECVD silicon dioxide is deposited at 160 °C, and subsequently patterned and etched via RIE to expose the base silicon. Trenches are then etched into the silicon via DRIE approximately 10 μm deeper than the first DRIE to allow for the parylene-filled trenches to be undercut. This undercut is achieved by exposing the wafer to xenon difluoride (XeF₂) gas, which isotropically etches silicon that is not protected with parylene. Finally, a short RIE is done to remove the remaining oxide on the surface. The process flow is shown graphically in figure 2.

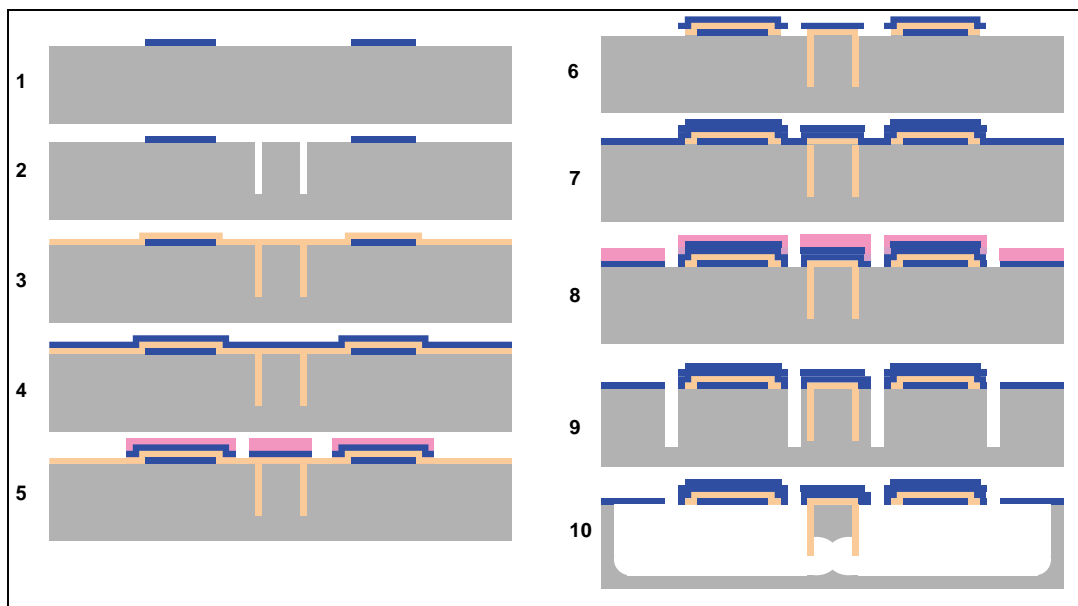


Figure 2. Parylene fabrication process: 1. Pattern (dummy) actuators; 2. Etch deep trenches; 3. Coat parylene; 4. Deposit oxide hard mask; 5. Pattern photoresist for parylene etch; 6. Etch parylene and photoresist; 7. Deposit additional oxide; 8. Pattern oxide, thin photoresist; 9. Etch deep trenches; and 10. XeF₂ release.

A labeled sample actuator/flexure/leg-link test structure is shown in figure 3 (2). The structures pictured in this report also include a D-Flexure, which is an added connection between the anchor and the leg-link (parallel to the flexure) that provides torsional stiffness.

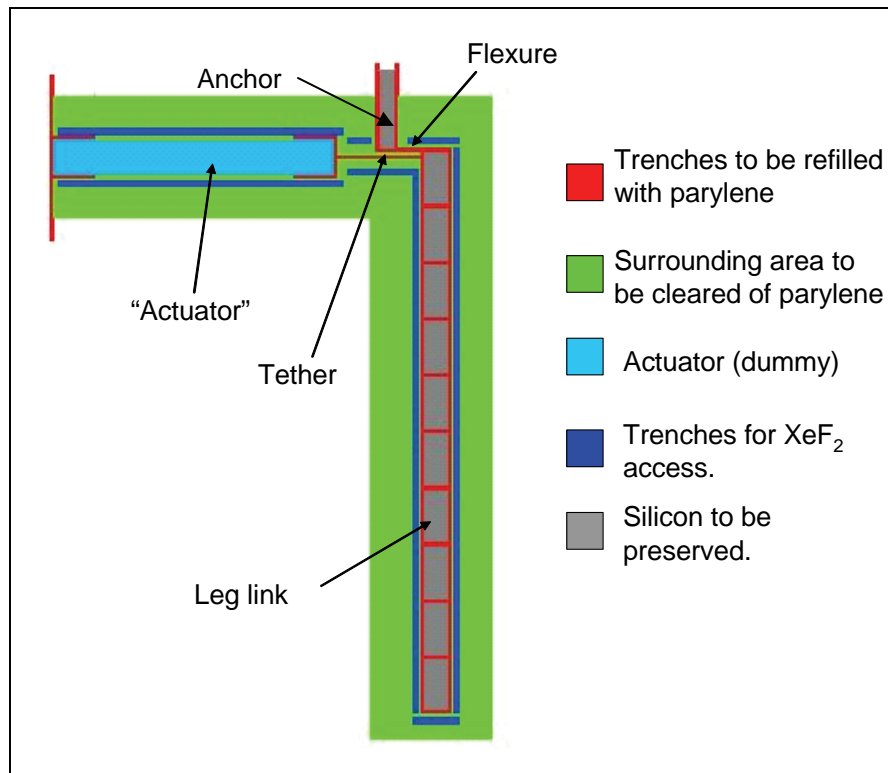


Figure 3. The sample actuator/flexure/leg-link test structure. In figures 4–8 the structures also contain a D-Flexure in parallel to the flexure.

These leg links are also combined in a series configuration in order to provide the large range of angular motion. This combined angular motion of approximately 45° of rotation at the joint mimics insect-like mobility.

3. Results and Discussion

Results from the initial testing of the process fall into four categories: trench junction failures, parylene adhesion and etching, trench analysis, and photolithography. These categories are discussed in depth below.

3.1 Trench Junctions

Observations of the first processed wafers indicate that over half of the structures exhibited defects at junctions where four trenches meet as seen in photographs from an optical microscope in figures 4 and 5.

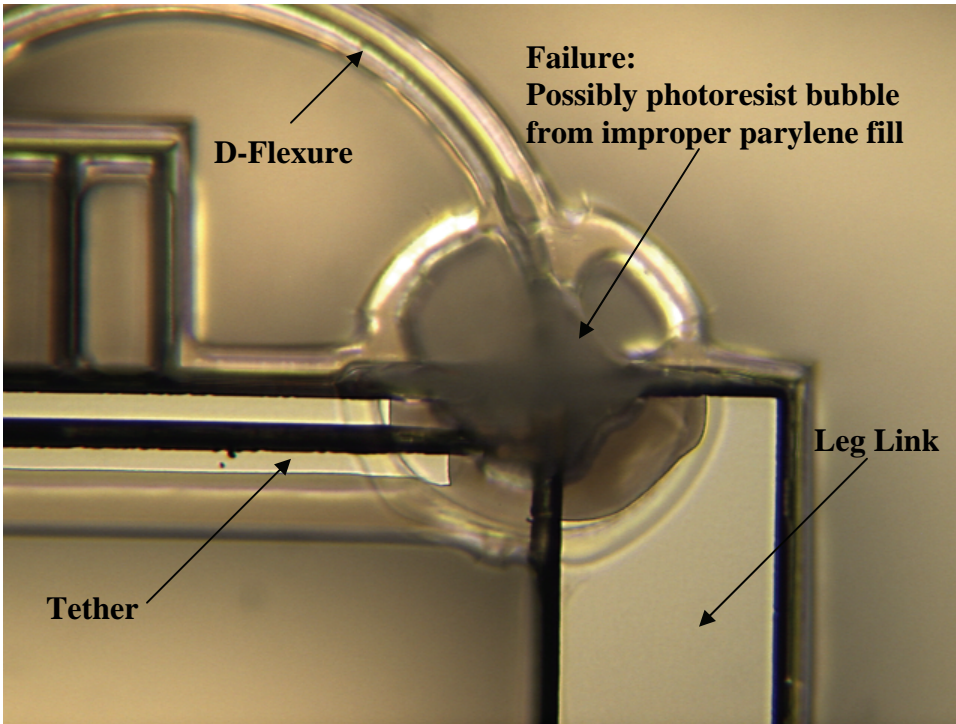


Figure 4. This photograph from the optical microscope illustrates failure at the junction between the flexure and the leg link, possibly from improper parylene fill or photoresist bubbles.

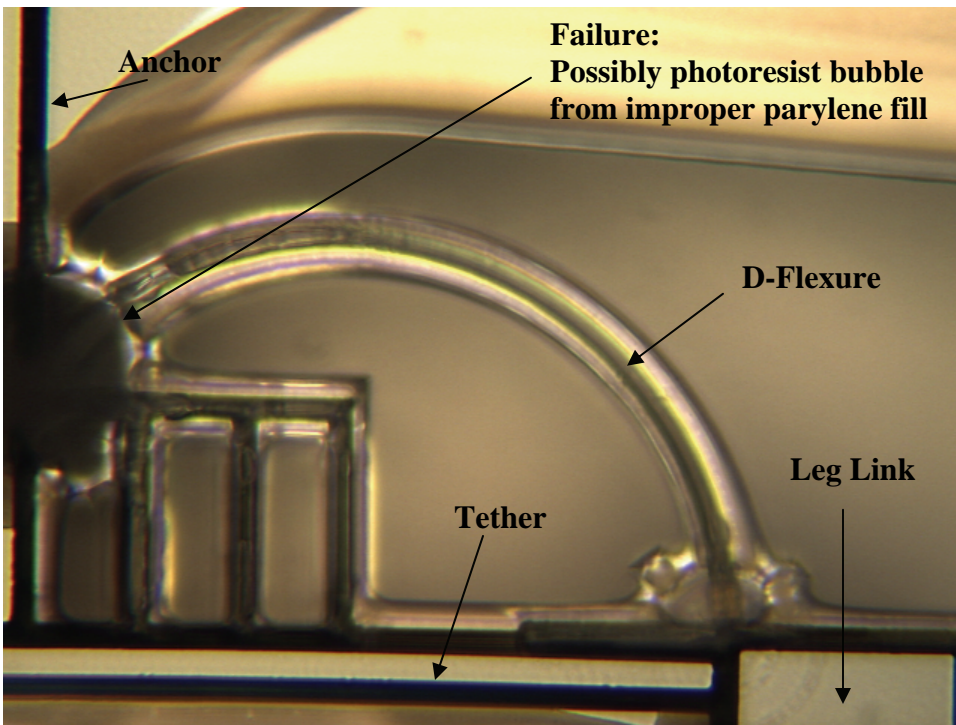


Figure 5. This photograph from the optical microscope illustrates a failure at the junction between the D-flexure and the anchor, possibly from improper parylene fill or photoresist bubbles.

The defects are of specific concern because these failures are occurring at connection points of the flexure, which are essential in providing a connection to the anchor, as well as creating torsional rigidity and in-plane flexibility. If this connection fails, then the leg link could be completely separated from the actuator or twist out of plane. Process or design changes are necessary to correct these issues. Options include depositing thicker parylene coatings to properly fill the junctions, decreasing the width of trenches near junctions, and avoiding four-trench junctions where possible.

Insight into the failure at the four-trench junctions may be seen immediately after parylene coating in figures 6 and 7, showing that the parylene did not fully coat the entire junction. These images indicate that a thicker parylene coating should be deposited to properly fill the entire trench at the junction intersections or a mask change should be made to decrease the width of the trenches near the intersections.

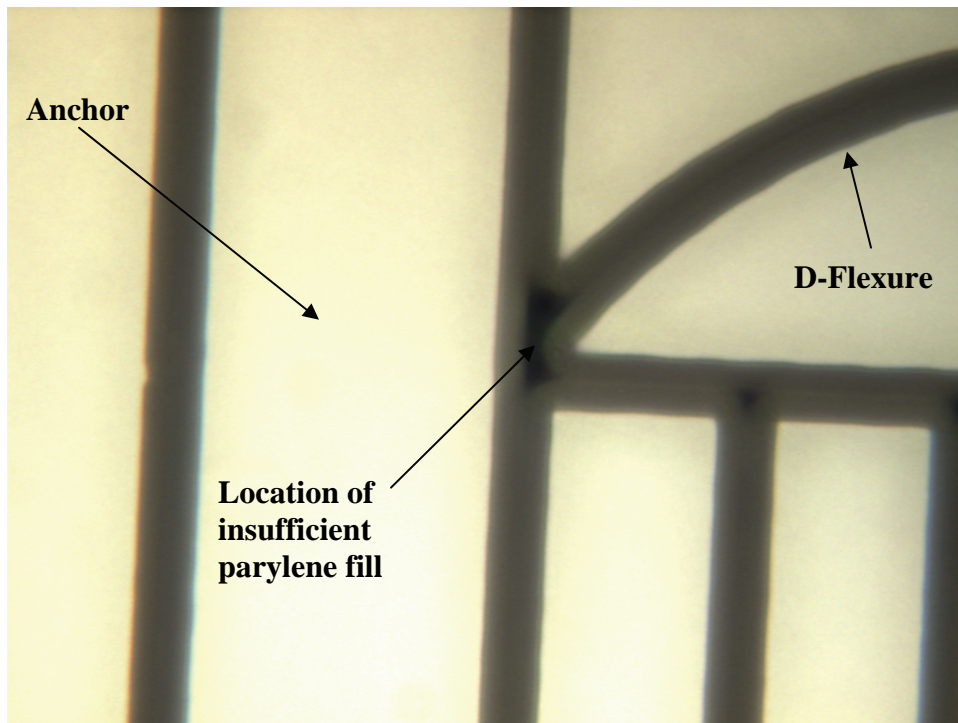


Figure 6. This photograph from the optical microscope shows insufficient parylene fill in the dark black areas near the four-trench junction at the anchor and D-Flexure intersection.

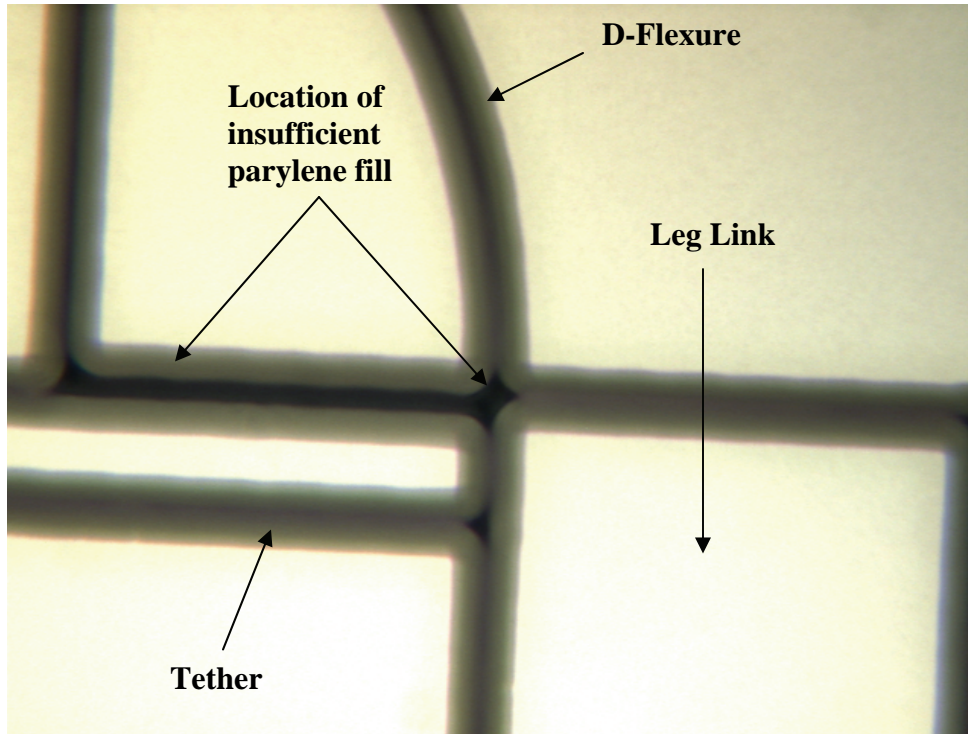


Figure 7. This photograph from the optical microscope shows insufficient parylene fill in the dark black areas near the D-Flexure-leg link four-trench junction.

3.2 Parylene Adhesion and Etching

Parylene adhesion to platinum and PZT was of initial concern as proper adhesion is critical to the success of the actuator joints. Parylene adhesion to platinum was tested utilizing a laminated composite consisting of silicon dioxide coated with a thin titanium layer and 85 nm of platinum. After patterning of the test actuators, parylene was deposited as with the silicon dioxide test actuators. The initial parylene coating on platinum proved successful with a uniform coating having the exact same appearance and characteristics as the coatings on silicon dioxide. In addition, a parylene coating was applied to a composite stack of SiO₂/Ti/Pt/PZT/Pt with thicknesses similar to the actuators used in reference 1. Similar to the previous results, the parylene coating was uniform without defects or signs of delamination.

Parylene etching has presented a problem in this process because the original methods of using Axcellis Downstream Asher resulted in more than 9 μm of parylene undercut due to the isotropic nature of the etching process. This undercut is more than 3 μm larger than the tolerable undercut in the design. For this reason, the etching process was changed to use an anisotropic RIE in order to prevent this excessive undercut (3). Using a Lam 590 parallel plate RIE system, the process showed considerable improvement with less than a 2 μm undercut. However, the process leaves behind residues on the exposed silicon surface, as seen in figure 8.

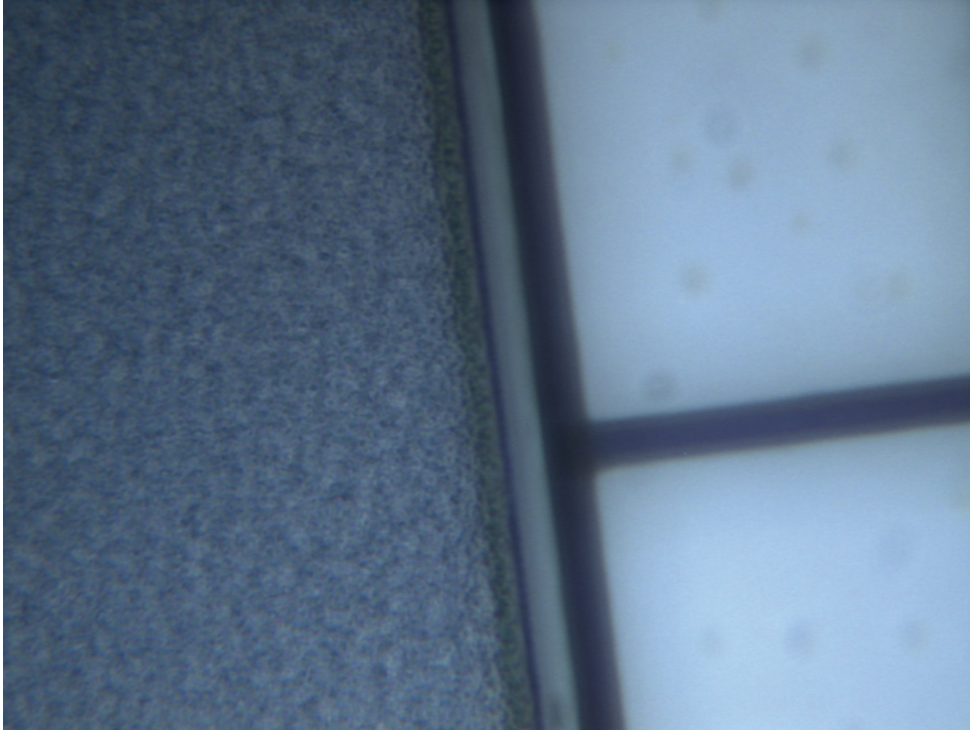


Figure 8. Surface residue on exposed silicon after anisotropic oxygen plasma RIE Lam 590.

At this time, it is unknown whether or not this residue will pose a problem with the final process steps. Further analysis needs to be done to determine if this is a significant issue.

After patterning the parylene, samples showed no immediate parylene delamination; however, after an hour or more, several samples began to delaminate. This delamination was seen on wafers with silicon oxide dummy actuators as well as wafers with PZT dummy actuators, so it is unclear if the dummy actuator material contributes at all to this delamination. Further investigation is needed in order to determine if the parylene coating and patterning process is time sensitive. Furthermore, since the parylene coating was done outside of the cleanroom, the delamination could also be attributed to the unclean environment or to the time between preparing the wafer surface with HMDS and actually depositing the parylene. The entire wafer was not delaminated and some of the test structures on the PZT coated wafer have been successfully released.

3.3 Trench Analysis

Proximity of trenches as well as trench width has an effect on trench depth and etch profile for silicon DRIEs performed with the Bosch process (4, 5, 6). In order to characterize this effect for our specific purposes, trenches spaced 420 μm apart (figure 9) and 76 μm apart (figure 10) were run through the same DRIE and were then filled with parylene, diced, and compared using the SEM.

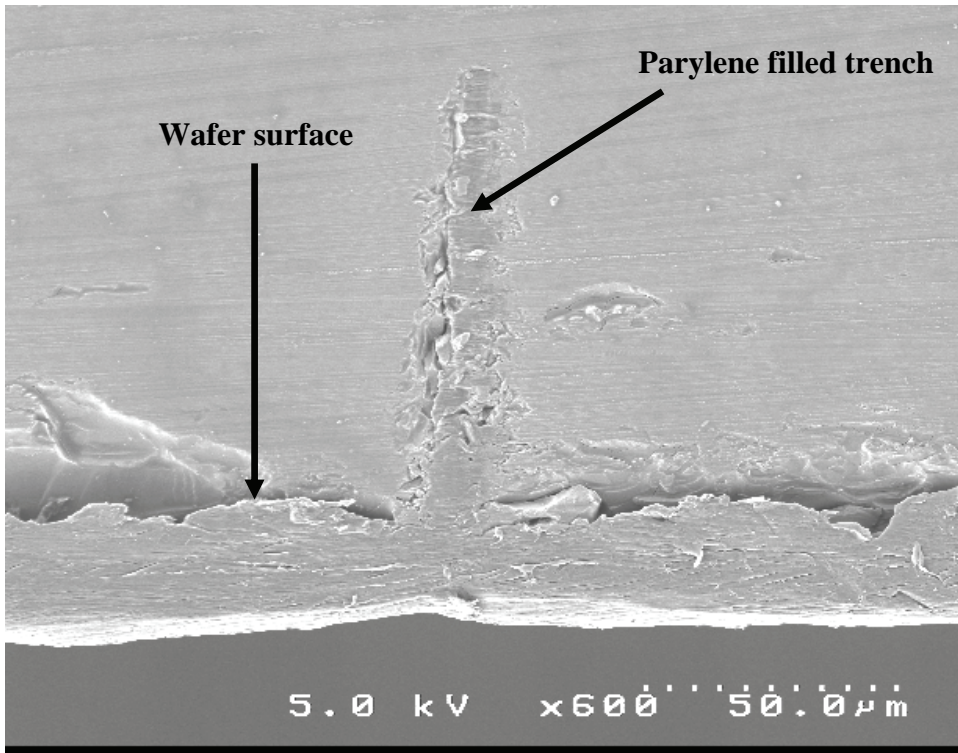


Figure 9. This photograph from the SEM shows a parylene filled trench 5 μm wide. The etch depth here is approximately 82 μm .

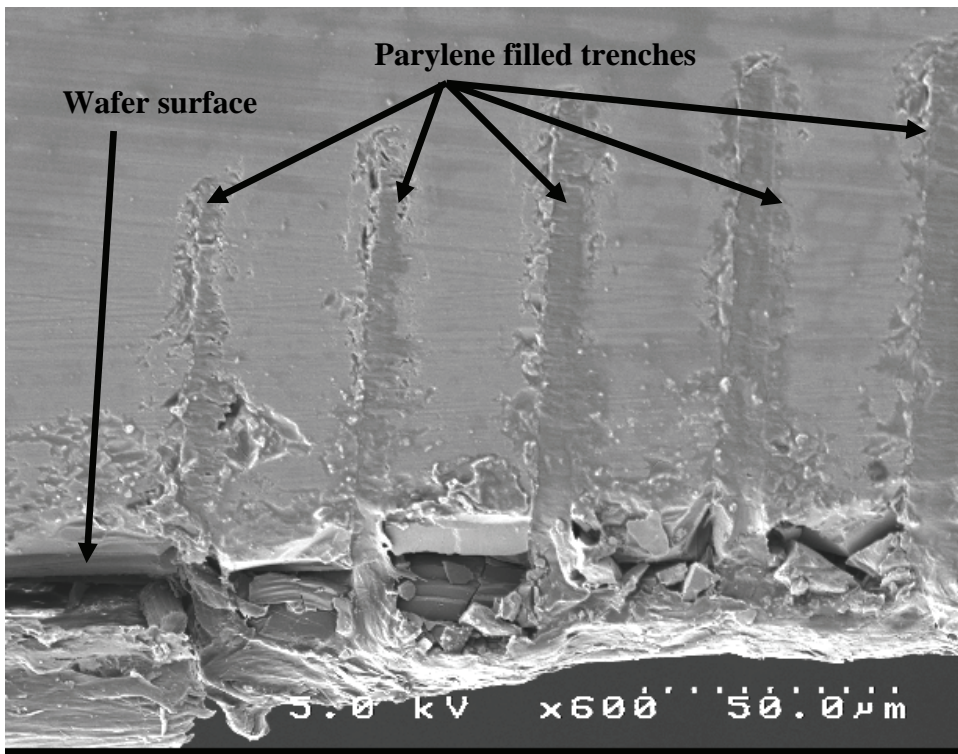


Figure 10. This photograph from the SEM shows the parylene filled trenches of widths of 3, 4, 5, 6, and 7 μm spaced 30 μm apart. The etch depth is approximately 76 μm for the 5 μm wide trench.

Measurements of these trenches show that for trenches within the range of 3–9 μm wide and 60–120 μm deep, trench depth is approximately linearly dependent on trench width and also offset by trench proximity by approximately 6 μm as seen in figure 11.

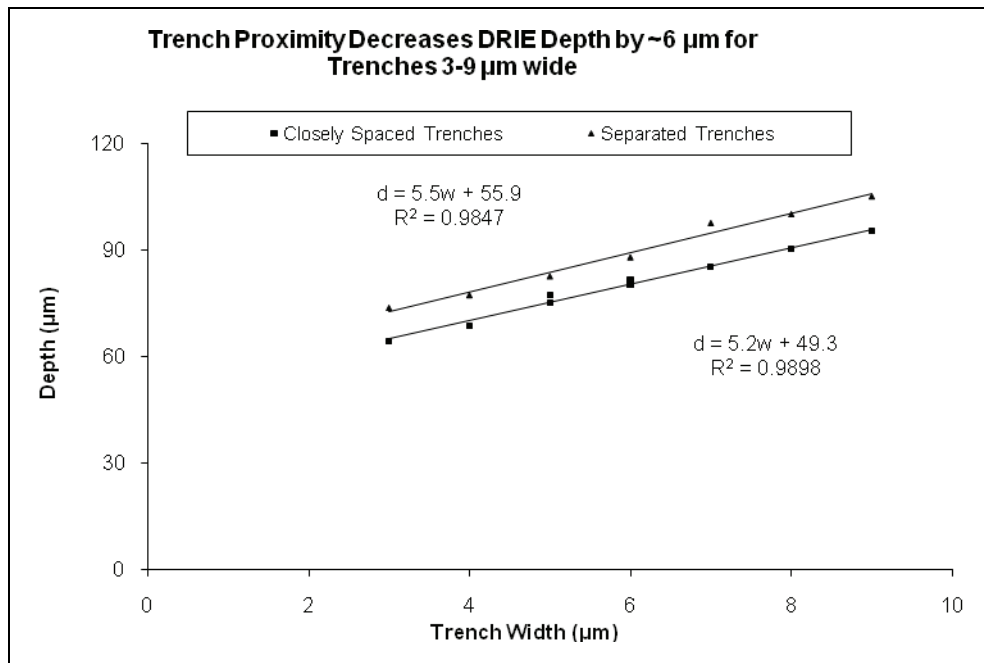


Figure 11. The graph shows that trenches that are close together result in more shallow etch profiles and that trench depth is linearly dependent on trench width within the range of etch.

Although the affect of trench proximity is small, it is still something that should be considered during design. It is especially important when considering placing trenches near large openings, which can locally deplete the etching species (4).

3.4 Photolithography

Several processing challenges occurred that were related to photolithography and will be described in this section. These challenges, though their effects were unfavorable, should be easily accounted for in subsequent processing.

During the last photolithography step, after the etching of parylene, three wafers were placed in acetone to remove photoresist due to insufficient coverage during the spinning of photoresist on the wafers. It appears that on these wafers, the acetone caused delamination at the etch fronts of the parylene-coated layer. To prevent delamination in future processing, the last photolithography step must be completed correctly on the first attempt as the photoresist cannot be removed without etching or delaminating the parylene coating. If photoresist must be removed, PRS3000 may work, but this has not been proven successful and it would be best if it could be avoided. A manual spin may be the best option for coating the wafer in this photolithography step in order to ensure good coverage over all of the topography on the wafer.

Finally, during the second DRIE, one of the wafers had been overetched. The photoresist was completely removed during the DRIE and the remaining parylene was removed during the DRIE and afterwards when the photoresist was supposed to be removed using a short oxygen plasma. In the original process flow, the photoresist was supposed to be thinned prior to the second DRIE; however, this step is not needed and can result in overetching of the structures.

4. Conclusions

From observations of previously processed wafers as well as wafers being currently processed, it is apparent that changes to the process are needed. First, the photoresist thinning step prior to the second deep silicon etch should be removed in order to prevent overetching. Second, the last photolithography step should be manually spun in order to ensure full coverage and avoid exposing the parylene to acetone or oxygen plasma, which can etch and cause delamination of the parylene. Third, in order to etch the parylene, an anisotropic RIE should be used to prevent undercut, followed by a downstream oxygen plasma etch to prevent the surface residue (if it proves to be problematic). Fourth, a thicker parylene coating should be deposited to successfully cover the four-trench junctions and prevent photoresist bubbles and trench junction failures. Finally, further work needs to be done to determine the cause for the delayed parylene delamination observed.

There are also design changes that may be made, such as eliminating four-trench junctions where possible. This mask change may be aided by the fact that the electrical interconnects are still being tweaked to prevent adding excessive stiffness.

Future work will also include duplicating the full processing on wafers with oxide dummy structures and determining yield, and eventually, conducting functional device testing.

5. References

1. Oldham, K.; Pulskamp, J.; Polcawich, R. G.; and Dubey, M. Thin-Film PZT Lateral Actuators with Extended Stroke. *J. MEMS* **2008**, *17*, 890–899.
2. Oldham, K. *Parylene Mechanisms for Integration with Piezoelectric Thin-Film Actuators*; ORISE final Report, 2008.
3. Meng, E.; Li, P.; Tai, Y. Plasma removal of Parylene C. *Micromechanics and Microengineering* **2008**, *18*.
4. Ayón, A. A.; Braff, R.; Lin, C. C.; Sawin, H. H.; Schmidt, M. A. Characterization of a Time Multiplexed Inductively Coupled Plasma Etcher. *Journal of The Electrochemical Society* **1999**, *146* (1), 339–349.
5. Ayón, A.A.; Zhang, X.; Khanna, R. Anisotropic silicon trenches 300-500 μ m deep employing time multiplexed deep etching (TMDE). *Sensors and Actuators* **2001**, *91*, 381–385.
6. Blauw, M. A.; Zijlstra, T.; van der Drift, E. Balancing the etching and passivation in time-multiplexed deep dry etching of silicon. *J. Vac. Sci. Tech. B* **2001**, *19* (6).

Acronyms

| | |
|------------------|---|
| ARL | U.S. Army Research Laboratory |
| DRIE | deep reactive-ion etching |
| HMDS | Hexamethyldisilazane |
| PECVD | plasma enhanced chemical vapor deposition |
| piezoMEMS | piezo-microelectromechanical systems |
| PZT | lead zirconate titanate |
| RIE | reactive ion etching |
| SEM | scanning electron microscopy |
| XeF ₂ | xenon difluoride |

| NO. OF COPIES | ORGANIZATION | NO. OF COPIES | ORGANIZATION |
|------------------|---|------------------|--|
| 1 ELEC | ADMNSTR DEFNS TECHL INFO CTR ATTN DTIC OCP 8725 JOHN J KINGMAN RD STE 0944 FT BELVOIR VA 22060-6218 | 1 | US ARMY RSRCH LAB ATTN AMSRD ARL SL EE M ADAMES BLDG 1624 RM 108 WHITE SANDS MISSILE RANGE NM 88002 |
| 1 | DARPA ATTN IXO S WELBY 3701 N FAIRFAX DR ARLINGTON VA 22203-1714 | 1 | US GOVERNMENT PRINT OFF DEPOSITORY RECEIVING SECTION ATTN MAIL STOP IDAD J TATE 732 NORTH CAPITOL ST NW WASHINGTON DC 20402 |
| 1 CD | OFC OF THE SECY OF DEFNS ATTN ODDRE (R&AT) THE PENTAGON WASHINGTON DC 20301-3080 | 1 | US ARMY RSRCH LAB ATTN AMSRD ARL CI OK TP TECHL LIB T LANDFRIED BLDG 4600 ABERDEEN PROVING GROUND MD 21005-5066 |
| 1 | US ARMY RSRCH DEV AND ENGRG CMND ARMAMENT RSRCH DEV AND ENGRG CTR ARMAMENT ENGRG AND TECHNLGY CTR ATTN AMSRD AAR AEF T J MATTS BLDG 305 ABERDEEN PROVING GROUND MD 21005-5001 | 1 | DIRECTOR US ARMY RSRCH LAB ATTN AMSRD ARL RO EV W D BACH PO BOX 12211 RESEARCH TRIANGLE PARK NC 27709 |
| 1 | US ARMY TRADOC BATTLE LAB INTEGRATION & TECHL DIRCTRT ATTN ATCD B 10 WHISTLER LANE FT MONROE VA 23651-5850 | 16 | US ARMY RSRCH LAB ATTN AMSRD ARL CI OK PE TECHL PUB ATTN AMSRD ARL CI OK TL TECHL LIB ATTN AMSRD ARL SE RL J PULSKAMP ATTN AMSRD ARL SE RL R POLCAWICH (9 copies) ATTN AMSRD ARL SE RL B. PIEKARSKI ATTN AMSRD ARL SE R P. AMIRTHARAJ ATTN IMNE ALC IMS MAIL & RECORDS MGMT ADELPHI MD 20783-1197 |
| 1 | PM TIMS, PROFILER (MMS-P) AN/TMQ-52 ATTN B GRIFFIES BUILDING 563 FT MONMOUTH NJ 07703 | | |
| 1 | US ARMY INFO SYS ENGRG CMND ATTN AMSEL IE TD F JENIA FT HUACHUCA AZ 85613-5300 | | |
| 1 | COMMANDER US ARMY RDECOM ATTN AMSRD AMR W C MCCORKLE 5400 FOWLER RD REDSTONE ARSENAL AL 35898-5000 | TOTAL: | 28 (1 ELEC, 1 CD, 26 HCS) |